Self-Spreading of Phospholipid Bilayer in a Patterned Framework of Polymeric Bilayer

Tamura, Fuyuko
Tanimoto, Yasushi
Nagai, Rurika
Hayashi, Fumio
Morigaki, Kenichi

(Citation)
Langmuir,35(45):14696-14703

(Issue Date)
2019-11-12

(Resource Type)
journal article

(Version)
Accepted Manuscript

Self-spreading of phospholipid bilayer in a patterned framework of polymeric bilayer

Fuyuko Tamura[1], Yasushi Tanimoto[2], Rurika Nagai[1], Fumio Hayashi[3], Kenichi Morigaki[1,2]*

1: Graduate School of Agricultural Science, Kobe University, Rokkodaicho 1-1, Nada, Kobe 657-8501, Japan

2: Biosignal Research Center, Kobe University, Rokkodaicho 1-1, Nada, Kobe 657-8501, Japan

3: Graduate School of Science, Kobe University, Rokkodaicho 1-1, Nada, Kobe 657-8501, Japan

*Corresponding author:

Kenichi Morigaki: E-mail: morigaki@port.kobe-u.ac.jp, Fax: +81-78-803-5941

Abstract

Phospholipid bilayers spontaneously spread on a hydrophilic substrate such as glass in aqueous solution due to the energetic gain of surface wetting. This process (self-spreading) was utilized to form a patterned model biological membrane containing reconstituted membrane proteins. A mechanically stable framework of polymerized lipid bilayer was first generated by the lithographic polymerization of a diacetylene phospholipid. Then, natural lipid membranes (fluid bilayers) were introduced into the channels between polymeric bilayers by the self-spreading from a phospholipid reservoir. The spreading velocity could be fitted into a slope of -0.5 in a double logarithmic plot versus time, due to the balance between spreading force and resistive drag. The preformed polymeric bilayer accelerated the spreading by the energetic gain of covering hydrophobic edges with lipid bilayer. At the same time, the domains of polymeric bilayer obstructed spreading, and the spreading velocity linearly decreased with their fractional coverage. Above the critical coverage of ca. 50%, self-spreading was completely blocked (percolation threshold), and fluid bilayer was confined in the polymer-free regions. Nonspecific adsorption of lipids onto the surface of polymeric bilayers was negligible, which enabled a heightened signal-to-background ratio in the reconstitution and observation of membrane proteins. Self-spread bilayers had a higher density of lipids than those formed by the spontaneous rupture of vesicles (vesicle fusion), presumably due to the continual supply of lipid molecules from the reservoir. These features give the self-spreading important advantages for preparing patterned model membranes with reconstituted membrane proteins.

1. Introduction

Substrate-supported model membranes are widely used to study the structural organization and physicochemical properties of the biological membrane by applying highly sensitive analytical techniques, such as surface plasmon resonance and quartz crystal microbalance. [1-3] However, creating a model membrane containing functional membrane proteins poses a major technological challenge. Supported model membranes are currently being generated most commonly by a process called vesicle fusion, in which vesicles adsorb onto the substrate surface, rupture into planar membrane patches, and fuse to form a continuous lipid bilayer. [4-6] Although this technique is widely used owing to its facile self-assembly process, there are technical issues such as formation of defects in response to the membrane environment changes. For example, reconstitution of membrane proteins from a detergent-solubilized state often causes defects due to the lipid solubilization by detergent micelles, and leads to nonspecific adsorption and aggregation of proteins.

An alternative approach to form a supported model membrane is the spontaneous spreading of a lipid bilayer on a hydrophilic surface from a reservoir of liquid crystalline lipid bilayers (self-spreading).[7-9] Since lipid molecules are continually supplied from the lipid reservoir, this technique is potentially useful for the formation of supported membranes that are suitable for reconstituting membrane proteins. In fact, the authors who originally reported this phenomenon have envisioned the concept of "self-healing membrane" as a thermodynamically stable model membrane on solid substrate. [8,9] Here, we describe the formation of a patterned model membrane by the self-spreading technique, in the presence of a preformed framework of polymeric bilayers. We previously

developed a methodology to generate a patterned membrane composed of polymeric and fluid lipid bilayers.[10,11] A patterned polymeric bilayer that is lithographically generated from a diacetylene phospholipid by UV irradiation acts as a template for incorporating natural (fluid) bilayers. We previously observed that formation of fluid bilayers by the vesicle fusion was accelerated in the presence of preformed polymeric bilayers due to the energetic gain of sealing hydrophobic bilayer edges with planar bilayer.[12] Although several lines of studies investigated self-spreading of lipids on patterned substrates,[9,13-16] its advantages towards the creation of model membranes containing membrane proteins have not been exploited. In the present study, we form a continuous lipid bilayer by self-spreading from a lipid reservoirs and discuss on its unique advantages compared to the more widely used vesicle fusion method.

2. Materials and methods

2.1 Materials

1,2-bis(10,12-tricosadiynoyl)-*sn*-glycero-3-phosphocholine (DiynePC), 1,2-dipalmitoyl-sn-glycero-3-phosphocholine (DPPC), Cholesterol, 1,2-dihexanoyl-*sn*-glycero-3-phosphocholine (DHPC-C6), and G_{M1} ganglioside (brain, ovine) (GM1) were purchased from Avanti Polar Lipids (Alabaster, AL). 1,2-Dioleoyl-*sn*-glycero-3-phosphocholine (DOPC) was purchased from NOF Corporation (Tokyo, Japan). 1,2-dihexadecanoyl-*sn*-glycero-phophoethanolamine (TR-PE), Laurdan, and cholera toxin subunit B-Alexa Fluor 488 conjugate (CTB-488) were purchased from Molecular Probes (Eugene, OR). Cy7-NHS-ester was from GE Healthcare (Piscataway, NJ). Sodium dodecyl sulfate (SDS), octyl-β-D-glucopyranoside (OG), glucose oxidase, catalase, glucose and sodium chloride were purchased from Nakalai Tesque (Kyoto, Japan). Bovine Serum Albumin (BSA) and cyclooctatetraene (COT) were purchased from Sigma-Aldrich (St. Louis, MO). Deionized water used in the experiments was ultrapure Milli-Q water (Millipore) with a resistance of 18.2 MΩ cm. Microscopy coverslips were from Matsunami (Osaka, Japan). Poly(dimethylsiloxane) (PDMS) was obtained from Toray Dow Corning (Silpot 184, Tokyo, Japan), and PDMS block was made by mixing the silicone elastomer and the curing agent with a ratio of 10:1 (w/ w).

2.2 Substrate cleaning

The substrates were cleaned with a commercial detergent solution, 0.5% Hellmanex/water (Hellma, Mühlheim, Germany), for 20 min under sonication, rinsed with deionized water, treated in a solution of NH_4OH (28%)/H_2O_2 (30%)/H_2O (0.05:1:5) for 10 min at 65 °C, rinsed extensively with deionized water, and then dried in a vacuum oven for 30 min at

80 °C. Before use, the substrates were further cleaned by the UV/ozone treatment for 20 min (PL16−110, Sen Lights Corporation, Toyonaka, Japan).

2. 3 Preparation of polymeric bilayer

Monomeric DiynePC was dissolved in deionized water at the final concentration of 3 mM together with DHPC-C6 (5 mol%). For preparing vesicle suspensions, the mixture was frozen in liquid nitrogen and thawed in water bath at 60 °C (five cycles). After the freeze-and-thaw, DiynePC suspension was homogenized by an ultrasonic homogenizer (Branson Sonifier 150, Branson Ultrasonics, Danbury, CT) at 60 °C (30 sec x 2 with 20 sec interval). DiynePC suspension was deposited onto a cleaned substrate on ice to immediately cool the membrane. [17] Polymerization of DiynePC bilayers was conducted by UV irradiation using a mercury lamp (SP-9, Ushio, Tokyo, Japan) as the light source. The applied UV intensity was typically 15 mW/cm^2 at 254 nm, and the irradiation dose was 2 J/cm^2, which was sufficient to form a fully cross-linked polymeric bilayer. The polymerization was conducted in a deionized water that was depleted of oxygen by purging with argon. Desired patterns were transferred to the DiynePC bilayer in the polymerization process by illuminating the sample through a mask (a quartz slide with a patterned chromium layer coating) which was placed directly on the DiynePC bilayer. After the UV irradiation, non-polymerized DiynePC molecules were removed from the substrate surface by immersing in 0.1 M SDS solution at 30 °C for 30 min and rinsing extensively with deionized water. The patterned polymeric bilayers were stored in deionized water in the dark at 4 °C.

2. 4 Introduction of fluid lipid bilayers by vesicle fusion and self-spreading

Lipids dissolved in chloroform were mixed either in a round-bottom flask or in a watch dish, dried under a stream of nitrogen, and subsequently dried further for at least 4 h in a vacuum desiccator (pressure: ca. 100 Pa). For preparing vesicle suspensions, the dried lipid films were hydrated in PBS overnight (the lipid concentration was 1 mM). Lipid membranes were dispersed by five freeze/thaw cycles, and the suspension was extruded by using Liposofast extruder (Avestin, Ottawa, Canada) with 100 nm polycarbonate membrane filter (10 times) and 50 nm polycarbonate filter (15 times). Extruded vesicles were applied onto a substrate having a patterned polymeric bilayer to form supported planar lipid bilayers (SPB). For the self-spreading experiments, a small amount of dried lipid was transferred from the watch dish to a PDMS block and stamped onto a substrate. The lipid film on the substrate was hydrated in 10 mM Tris buffer solution (pH7.6) containing 100 mM NaCl at room temperature. The spreading bilayer was monitored with TR-PE in the lipid film.

The spreading kinetics was analyzed as previously reported. [7] The driving force of self-spreading is the gain of free energy by hydration and van del Waals forces, W_A (J/ m^2), whereas dissipation of energy by the dragging force on the surface decelerates the spreading. The balance between these factors determines the spreading velocity as follows:

$$W_A = \gamma_h L(t) v(t), \qquad (1)$$

where γ_h is a drag coefficient (Ns/ m^3), L(t) is a spreading distance (m) at time *t* (s), and v(t) is spreading velocity (m/ s). Since the lipid bilayer edges expand in one direction at the rim of a large lipid bilayer patch and lipid bilayers in line patterns, we can define the one-dimensional (1D) spreading velocity (m/s) by dividing the 2D spreading area velocity (m^2/s) with a unit width. Considering that $v(t) = dL(t)/ dt$, the equation can be integrated to

$$\log v(t) = \frac{1}{2}\log \beta - \frac{1}{2}\log t, \qquad (2)$$

where $\beta = W_A/2\gamma_h$ is the spreading coefficient (m^2/ s). The spreading velocity v(t) decreases with t, showing a slope of -0.5 in the double logarithmic plot. In Equation (1), γ_h represents the hydrodynamic shear flow, and can be estimated from the thickness of water layer between the bilayer and the substrate d_w (m) and the viscosity of water η_w (kg/ ms^2) using the following equation

$$\gamma_h = \eta_w/d_w. \qquad (3)$$

W_A can be obtained from β by the following equation

$$\beta = \frac{W_A d_w}{2\eta_w}, \qquad (4)$$

enabling to estimate the energetic gain of the self-spreading process.

2. 5 Fluorescence microscopy

Fluorescence microscopy observation was performed using an inverted microscope (IX-73, Olympus, Tokyo, Japan) equipped with a xenon lamp (UXL-75XB, Olympus), a 20× objective (NA 0.75) or 100× objective (NA 1.40), and a CMOS camera (Orca 4.0, Hamamatsu Photonics, Hamamatsu, Japan), and an image intensifier (C9016-05, Hamamatsu Photonics, Hamamatsu, Japan), except for the observation of reconstituted rhodopsin (*vide infra*). Two types of filter sets were used for observing the self-spreading: (1) excitation 470−490 nm/emission 510−550 nm (green fluorescence) and (2) excitation 545−580 nm/emission >610 nm (red fluorescence). The images were analyzed by ImageJ.

2. 6 Membrane viscosity/ hydration analysis

Membrane viscosity and hydration levels were microscopically characterized using an

environmentally sensitive fluorophore Laurdan. [18,19] The lipid composition and lipid packing impact the local membrane hydration levels, causing changes in the polarity-sensitive dye Laurdan fluorescence spectrum and lifetime values. [20] Laurdan emits fluorescence from at least two excited states, *i.e.* the locally excited state and the internal charge transfer state. The latter causes the reorientation of surrounding water molecules to align with the Laurdan dipole moment (solvent relaxation), consuming the energy of excited Laurdan molecules so that the emission is shifted to a longer wavelength (red-shifted emission). Laurdan displays a varying mixture of intrinsic and red-shifted fluorescence depending on the number of the surrounding water molecules, which can be used to assess the lipid environment in membranes. For the spectral analysis of Laurdan, fluorescence is typically collected at two wavelength, and the normalized difference between the two emission intensities known as the general polarization (GP) is calculated using the following equation

$$\mathrm{GP} = \frac{I_1 - I_2}{I_1 + I_2}, \qquad (5)$$

where I_1 and I_2 correspond to the intensities of intrinsic and red-shifted fluorescence, respectively. In the present study, planar bilayers containing 1 mol% of Laurdan were formed by vesicle fusion and self-spreading. Fluorescence of Laurdan was excited in the wavelength range of 360-370 nm, and emission was collected in two wavelength ranges, 420-460 nm (intrinsic fluorescence: $\lambda_{420\text{-}460}$) and 495-540 nm (red-shifted fluorescence: $\lambda_{495\text{-}540}$). In order to microscopically obtain GP values, we used the following equation, in which G value was the correlation factor between microscopic observations and more conventional spectroscopic data at two wavelength:

$$\mathrm{GP} = \frac{I_{420-460} - G * I_{495-540}}{I_{420-460} + G * I_{495-540}} \qquad (6)$$

G was obtained by the following equation using Laurdan fluorescence of DOPC vesicle suspensions measured both spectroscopically and microscopically. [21]

$$G = \frac{I^{ref}_{420-460} * (1 - GP^{ref})}{I^{ref}_{495-540} * (1 + GP^{ref})} \qquad (7)$$

where $I^{ref}_{420-460}$ and $I^{ref}_{495-540}$ are the intensities in the microscopic images, and GP^{ref} is the GP value obtained from the spectroscopic measurements of the same intensity regions (i.e. 420-460 nm and 495-540 nm). By definition, the spectroscopic and microscopic GP values are identical for the DOPC vesicles. We used thus obtained G value to analyze the membrane environment of planar bilayers.

2.7 Reconstitution of rhodopsin

Rhodopsin (Rh) was obtained from the rod outer segment (ROS) in the retinas of bullfrogs (*Rana catesbeiana*) and purified as described previously. [22,23] Briefly, ROS membranes were washed with a hypotonic buffer (5 mM Tris-HCl, 5 mM dithiothreitol, pH7.5), and solubilized with 50 mM OG in buffer A (20 mM HEPES, 1 mM $MgCl_2$, 120 mM NaCl, pH7.5), and Rh was purified with Con A-Sepharose column (Amersham Pharmacia Biotech AB). Approximately 4 mg/mL of Rh was obtained in buffer A containing 30 mM OG. Fluorescence-labeling of Rh was done as follows under IR illumination. ROS containing 50 nmole Rh was washed with 1 mL of 10 mM MOPS buffer (pH 7.5) (containing 60 mM KCl, 30 mM NaCl, 5 mM $MgCl_2$, 5 mM dithiothreitol, 5 μg/ mL aprotinin, 2 μg/ mL N-[N-(L-3-Trans-carboxirane-2-carbonyl)-L-leucyl]-agmatine (E-64), 2 μg/ mL leupeptin) by ultracentrifugation (452,000g, 5 min at 4 °C) three times. ROS suspension in MOPS buffer was mixed with Cy7-NHS dissolved in dimethyl sulfoxide (Rh/ Cy7-NHS = 1:20). Reaction was proceeded for 2 min at 0 °C, and stopped by adding 10 μmole of glycine. Cy7-labeled ROS was washed with 20 mM HEPES buffer (pH7.5) containing 1 mM $MgCl_2$ and 120 mM

NaCl by ultracentrifugation three times, and resulting pellet was solubilized with 0.1 mL of 100 mM OG in HEPES buffer. Following ultracentrifugation (65,000 g, 60 min at 4 °C), supernatant was applied to Con A-Sepharose column (0.5 mL) equilibrated with HEPES buffer containing 30 mM OG. Cy7-labeled Rh (Cy7-Rh) was eluted with 250 mM methyl α-D-mannoside in HEPES buffer with 30 mM OG. Thus obtained Cy7-Rh was reconstituted into a pre-formed planar bilayer by the rapid dilution of solubilized Rh molecules. [24] Cy7-Rh was diluted with 30 mM OG in phosphate buffer saline (PBS: 0.01 M sodium phosphate buffer with 0.15 M NaCl, pH7.0) to the final concentration of 76 nM. 10 μL of the diluted solution was quickly mixed with 400 μL of PBS in the chamber. For rapidly incorporating Rh into the bilayer, the solution was vigorously stirred with a magnet. Furthermore, vesicle suspensions of DOPC were pre-added to the PBS solution (total lipid concentration: 0.75 mM) to deplete excess Rh molecules. Reconstituted Cy7-Rh was observed by the total internal reflection fluorescence microscopy (TE2000-V; Nikon, Tokyo, Japan) equipped with a near-infrared laser diode (SL750 nm 100T; Shanghai Sauk Kaser, Shanghai, China). Images were acquired by an electron-multiplying charge-coupled device camera (C9100-12; Hamamatsu Photonics, Hamamatsu, Japan) at temporal resolution of 33 frames s^{-1} and spatial resolution of 76 nm $pixel^{-1}$. To minimize photobleaching and blinking during the observation, 2.5 μg/mL glucose oxidase, 2.5 μg/mL catalase, 70 μg/ mL glucose, and 10 mM COT were added.

3. Results and discussion

3.1 Self-spreading in the patterned framework of polymeric bilayer

Figure 1(B) shows the fluorescence micrographs of spreading bilayers (DOPC with 1% TR-PE) on glass in the presence of stripe-patterned polymeric bilayers. The brightest region at the bottom of images was the lipid reservoir, from which single bilayers spread upon hydration. The edge of bilayers moved forward with time (the fluorescence intensity profiles are shown in Supporting Information, Figure S1), while the spreading bilayers were strictly confined in the regions between polymeric bilayer. The edge of the spreading bilayer had a slightly brighter fluorescence of TR-PE due to the accumulation of sterically bulky Texas-Red chromophore. [8] As we plotted the distance of lipid bilayer edge from the reservoir, the spreading velocity decreased with time (Figure 1(C)). [7] The decrease in velocity was interpreted as a result of dragging the membrane by the friction with the water layer and substrate. According to this model, the double logarithmic plot of spreading velocity versus time has a linear relation with the slope of -0.5 (Figure 1(D)). From the fitting we obtained the spreading coefficient $\beta = 1.11 \times 10^{-11}$ (m^2/ s) and free energy gain W_A = 8.97 x 10^{-6} (J/m^2), which is close to the previously reported values. [7] Importantly, the spreading bilayers retained lateral mobility of lipid molecules, as qualitatively investigated by the fluorescence recovery after photo-bleaching (Figure 1(E)). The edge of bleached spot became unclear with time, clearly demonstrating the lateral mobility of TR-PE (and hence DOPC) molecules.

To assess the influences of the polymeric bilayer framework on the self-spreading, the velocities were compared for a non-patterned substrate (bare glass) and patterned bilayers with various stripe width (Figure 2). The spreading energy W_A was larger for patterned

substrates ((6.61 ± 1.52) $\times 10^{-6}$, (9.09 ± 0.38) $\times 10^{-6}$ and (9.16 ± 0.40) $\times 10^{-6}$ J/m^2 for 200 μm, 50 μm and 20 μm stripes, respectively) compared with a bare glass was ((5.85 ± 0.43) $\times 10^{-6}$ J/m^2), indicating that the existence of polymeric bilayer enhanced the spreading of bilayers. One potential source of acceleration is the energetic gain due to coverage of polymerized lipid bilayer edges by the self-spreading lipid membrane. Since the contact of polymeric bilayer edges and water is energetically unfavorable, covering the edges with a lipid bilayer should result in a free energy gain. We previously observed microscopically that formation of planar bilayers from adsorbed vesicles was initiated preferentially at the edges of polymeric bilayers and propagated to the center of polymer-free areas. [12] A study using a patterned hydrophobic surface has also shown that lipid spreading was accelerated on hydrophobic surfaces. [25] We estimated the energetic gain of bilayer edge sealing from the interfacial energy of polymeric bilayer edge per unit length λ (line tension). Assuming that the interfacial free energy between hydrophobic acyl chains and water (γ_i) is 50 mJ/m^2, [26,27] and the thickness l of the hydrophobic section of polymeric bilayer is 3 nm, [11] we obtain the line tension λ as follows:

$$\lambda = l\gamma_i = 1.5 \times 10^{-7} \text{ mJ/m} \qquad (8)$$

This energetic gain is added to the spreading energy on the bare glass $W_{A\ (bare\ glass)}$. Therefore, the total spreading energy in the presence of polymeric bilayer $W_{A\ (pattern)}$ can be expressed as follows:

$$W_{A\ (pattern)} = W_{A\ (bare\ glass)} + \lambda \times N_{edge} \quad (9)$$

Here, N_{edge} is the density edges, which is inversely proportional to the line width. The simulated $W_{A\ (pattern)}$ is plotted versus N_{edge} (Supporting Information, Figure S2 red line). The estimated values agree favorably with the experimental results for the stripe width of 200μm and 50μm corroborating the premise that hydrophobic edge energy is

contributing to the faster self-spreading. On the other hand, the experimentally obtained value for 20μm stripes deviated from the estimation. Though the reason for this deviation is at present not clear, one plausible explanation is partial coverage of the glass surface with polymeric bilayer domains, since parallel line patterns with a small line interval tended to cause partial polymerization of the protected area. We found that presence of polymeric bilayer domains obstructed the spreading of fluid bilayers (*vide infra*).

3.2 Obstructed self-spreading in the presence of polymerized bilayer domains

DiynePC bilayers polymerize as domains with the average size of ca. 30 nm. [11] The surface coverage of polymeric bilayer domains can be controlled by the UV dose applied to the polymerization. We can generate polymeric bilayer domains that partially cover the surface, and combine them with fluid lipid bilayer, forming a nanometric composite membrane of polymeric and fluid bilayers. Since such composite membranes are a useful platform for sorting membrane lipids and proteins, we investigated the self-spreading in the presence of polymeric bilayer domains that partially cover the surface. Figure 3(A) shows the spreading lipid bilayer in the polymer free region (R_0) and partially polymerized region (R_1). Spreading of bilayer in R_1 was retarded compared with R_0. The spreading velocities in R_1 were analyzed in the middle of wide stripes (200 μm), where the effect of boundaries was negligible. The double logarithmic plot of spreading velocity versus time had a linear relation with the slope of -0.5 (Figure 3(B)). The spreading coefficient linearly decreased with the polymer fraction (coverage of the surface with polymeric bilayer) and reached zero at about 50% coverage of the surface by polymeric bilayer domains. This behavior is similar to the obstructed lateral diffusion in two dimensional fluid systems, which has been extensively studied using the percolation model. [28,29] In a composite membrane of

polymeric and fluid lipid bilayers, we previously demonstrated that the lateral mobility of lipid molecules linearly decreased with the coverage of polymeric bilayer domains, reaching the percolation transition at ca 40% coverage. [11] The linear decline and percolation clearly demonstrate that polymeric bilayer domains act as obstacles for the spreading of lipid bilayers, as was previously reported for the periodic array of metallic nanoarchitecture generated by nanosphere lithgraphy. [16]

3.3 Phase separation of spreading bilayers

Biological membrane consists of heterogeneous and dynamic mixture of lipids and proteins, such as raft.[30,31] The heterogeneous lipid domains have been extensively studied using the coexistence of liquid ordered (L_o) and liquid disordered (L_d) phases in model membranes including giant vesicles and supported membranes. [24,32-36] A patterned bilayer having partially polymeric and polymer-free bilayer regions can induce patterned separation of L_o/ L_d phases. [37] From a mixed lipid membrane (DOPC/ DPPC/ cholesterol (1:1:1)), the L_o phase (DPPC, cholesterol) is accumulated in the polymer-free region, whereas the L_d phase (DOPC) is accumulated in the partially polymeric region. L_o domains are excluded from the partially polymeric regions presumably due to the higher energetic penalty of height mismatch between polymeric and fluid bilayers, owing to the higher bending elasticity of L_o domains. Since this phenomenon is potentially useful for evaluating the affinity of membrane-bound molecules to raft, [24] we studied the simultaneous phase separation of a mixed lipid membrane during self-spreading. The spreading bilayers were homogeneous 10 minutes after the hydration as observed by the fluorescence microscopy (Figure 4). The bilayer edge proceeded slightly farther in the

polymer-free region (R_0) compared with the partially polymeric region (R_1) due to obstructed spreading in R_1. After incubating for 1 day, the spread bilayer showed macroscopic phase separation of the L_o and L_d phases (Figure 4). In the farthest region from the reservoir, fluorescence of TR-PE was observed primarily in R_0 ((a) in Figure 4). In the intermediate region, TR-PE was observed both in R_0 and R_1 ((b) in Figure 4), with the fluorescence intensity higher in R_0. In the vicinity of lipid reservoir, TR-PE was observed mostly in R_1 ((c) in Figure 4). As we applied a marker of the L_o domains, cholera toxin subunit B-conjugated with AlexaFluor-488 (CTB-488), it was found mostly in R_0 near the lipid reservoir (c), and not in the regions farther away from the reservoir ((a) and (b)). There results indicate that L_o domains containing G_{M1} was accumulated in the polymer-free region near the lipid reservoir. Segregation of L_o and L_d domains in a spreading bilayer was previously described. [38] Slower spreading of L_o domains is presumably due to a higher frictional coupling (i.e. dragging effect). [8] The obtained results demonstrated that the self-spreading process is accompanied with a macroscopic separation of lipid phases, which is potentially useful as a means of separating lipids and proteins in the biological membrane.

3.4 Lipid density of supported membranes formed by self-spreading

We evaluated the lipid-packing properties of model membranes formed by self-spreading using a polarity-sensitive dye 2-dimethylamino-6-lauroylnaphthalene (Laurdan). The general polarization (GP) values were obtained from microscopic images acquired at two emission wavelength ranges, $\lambda_{420\text{-}460}$ and $\lambda_{495\text{-}540}$ (Figure 5). GP of vesicle suspensions was obtained by spectroscopic and microscopic methods and used as the standard reference for determining the correction factor G to be 0.179. The GP values of vesicle

suspensions, supported membrane prepared by vesicle fusion and self-spreading were 0.223 ± 0.010, 0.192 ± 0.005 and 0.270 ± 0.009 (means ± standard error), respectively (Figure 5(B)). Supported membrane from self-spreading had a significantly higher GP value compared with those from vesicle fusion, indicating a higher packing of lipid molecules. The heightened lipid packing of self-spread bilayers in comparison with those formed by vesicle fusion presumably stems from the fact that the self-spread bilayers are connected with lipid reservoirs that continually supply lipid materials. In contrast, vesicle fusion is a rapid, non-equilibrium transformation of spherical vesicles into a planar bilayer, in which adsorbed lipid vesicles first accumulate on the surface and then rupture rapidly in a catastrophic manner. [6,39] The rapid mutual fusion of planar bilayer patches to minimize the line tension should lower the lipid density by laterally stretching the bilayer membranes. The higher lipid packing in planar bilayers is potentially advantageous for constructing model membranes, because the membrane is less susceptible to defects formation.

3.5 Reconstitution of membrane proteins into the self-spread bilayer

A major technical challenge for supported model membranes is the reconstitution of membrane proteins. One approach is to reconstitute detergent-solubilized membrane proteins into a preformed lipid membrane. However, this method has a relatively narrow working window, since detergents can destabilize the lipid membrane. For assessing the utility of self-spread lipid bilayer as a model system containing membrane proteins, we reconstituted Cy7-labelled rhodopsin (Cy7-Rh) from bullfrogs (*Rana catesbeiana*). Solubilized Cy7-Rh (OG 30 mM) was added to a pre-formed planar bilayer to reconstitute by the rapid dilution. [24] We observed the lateral diffusion of single Cy7-Rh molecules

(Figure 6 and Supporting Movie 1 and 2). As a comparison, we reconstituted Cy7-Rh also into a planar bilayer formed by vesicle fusion. Mobile Cy7-Rh was observed in the fluid membranes for both conditions. In the case of lipid membranes prepared by vesicle fusion, lipids adsorbed onto the polymeric bilayer, and bright spots of lipid aggregates were observed both in the fluid and polymeric bilayer regions. Lipids on the polymeric bilayer was due to the nonspecific adsorption of vesicles during the vesicle fusion process. As a result of adsorbed lipids, more immobile Cy7-Rh molecules were observed on the polymerized bilayer for the patterned bilayer prepared by vesicle fusion. The aggregates in the fluid bilayer region may be induced by destabilization of the lipid membrane during the reconstitution process, since we incubated detergent-solubilized Cy7-Rh in the presence of vesicles in the aqueous phase. The same reconstitution process apparently did not cause lipid heterogeneity in the case of fluid bilayers prepared by self-spreading. These observations underline two advantages of self-spreading for reconstituting membrane proteins. First, nonspecific adsorption of lipids and proteins onto the patterning framework of polymeric bilayers is effectively suppressed, partially because the self-spread bilayers form exclusively in the polymer-free regions, contributing to a higher signal-to-background ratio. Second, fluid lipid bilayers formed by self-spreading is less prone to aggregation, presumably due to the fact that lipid molecules are continuously supplied from the lipid reservoir. Although a higher packing density of lipid bilayers as observed in 5 should increase the energetic barrier of protein insertion into the membrane, suppressed aggregation and defects formation are important for reconstituting a wider variety of membrane proteins, especially for those requiring specific detergents to preserve the functions during the solubilization/ reconstitution processes.

4. Conclusions

We formed a patterned lipid bilayer by utilizing the self-spreading phenomenon in the framework of patterned polymeric bilayers. The heightened spreading coefficients in the presence of polymeric bilayers indicated that the hydrophobic edges of polymeric bilayer enhanced the spreading to reduce the line tension. At the same time, polymeric bilayer domains in partially polymeric bilayer obstructed the spreading, retarding the spreading proportionally with the surface coverage of polymeric bilayer domains and reaching the percolation at the coverage of ca. 0.5. This phenomenon also contributed to the confinement of fluid bilayers in the polymer-free regions, with negligible nonspecific adsorption of lipids on the surface of polymeric bilayers. The confined membrane formation improved the signal-to-background ratio in the reconstitution and observation of membrane proteins. Another important observation in the present study was the heightened lipid packing in self-spread bilayers compared with those formed by vesicle fusion, most likely owing to the fact that lipid molecules can be continually supplied from the lipid reservoir. These features give the self-spreading important advantages for preparing patterned model membranes, especially for reconstituting membrane proteins, compared to the more widely used vesicle fusion method. Another unique observation is the macroscopic phase separation of a lipid bilayer having multiple lipid compositions, which can be used for sorting membrane-bound molecules according to the affinity to L_o and L_d regions. Furthermore, lipid bilayers can be stored in a dried state until use, which should be beneficial in biomedical applications of chemically unstable lipid membranes. Although patterned spreading has been studied in a number of systems [9,13-16] and "self-healing membrane" has been envisioned, [8,9] these unique advantages have remained unexplored so far. Therefore, we envisage that self-spreading in combination with the

preformed framework of polymeric bilayer provides a versatile methodology for preparing model membranes with heightened functionality and stability.

Supporting Information Available.

The Supporting Information is available free of charge on the ACS Publications website: Fluorescence intensity profiles of spreading bilayers at varied time after the hydration, plot of simulated $W_{A\,(pattern)}$ versus N_{edge}, and movies of reconstituted Cy7-Rh molecules.

Acknowledgements.

This work was supported by Grant-in-Aid for Scientific Research from Japan Society for the Promotion of Science (#17H03666). We thank Dr. Shohei Maekawa (Graduate School of Science, Kobe University) for supporting us with his lab infrastructures. Discussion with Dr. Kazuaki Furukawa (Meisei University) is appreciated.

Figures:

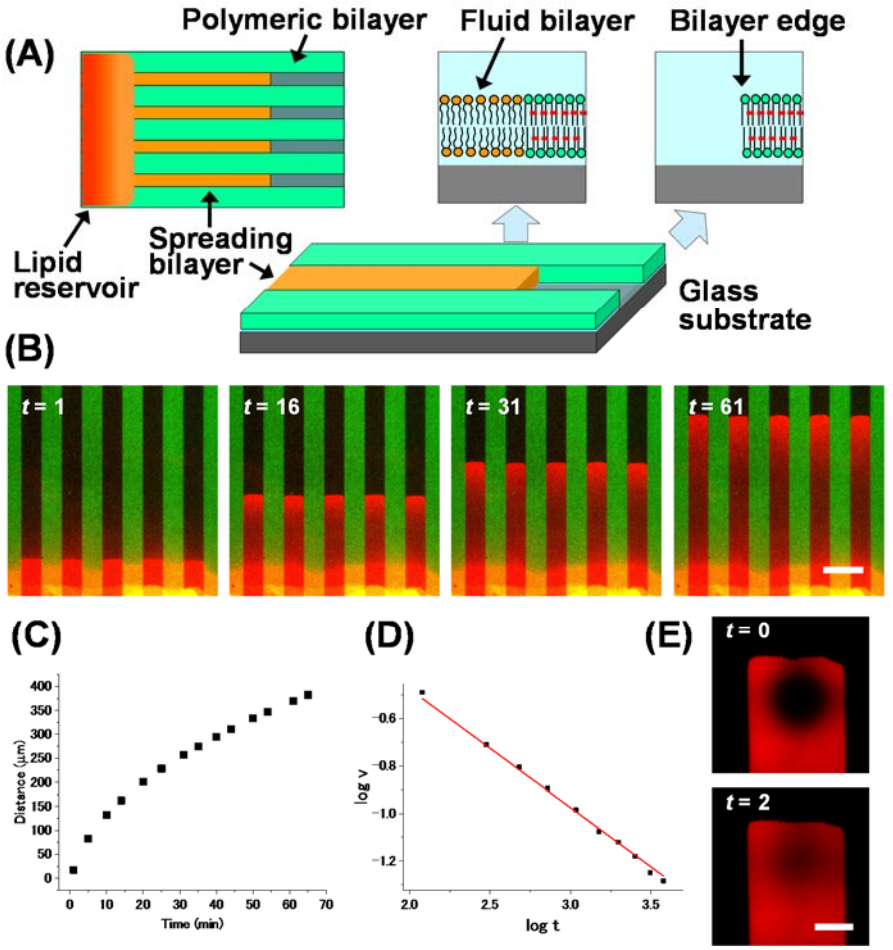

Figure 1: Bilayer spreading into the lipid-free channels between polymeric bilayers. (A) Schematic of the patterned bilayer spreading. (B) Fluorescence micrographs of self-spreading bilayers (DOPC/TR-PE) at varied time after the hydration (t: min). The red and green fluorescence were from DOPC/TR-PE and polymeric bilayers, respectively. The scale bar corresponds to 100 μm. (C) Plot of the spreading distance as a function of time (min). (D) Double logarithmic plot of the spreading velocity (μm/sec) vs time (sec). The red line is the linear fitting of the data points with the slope of -0.5. (E) Fluorescence recovery after partially photobleaching the membrane (t: min). The scale bar corresponds to 20 μm.

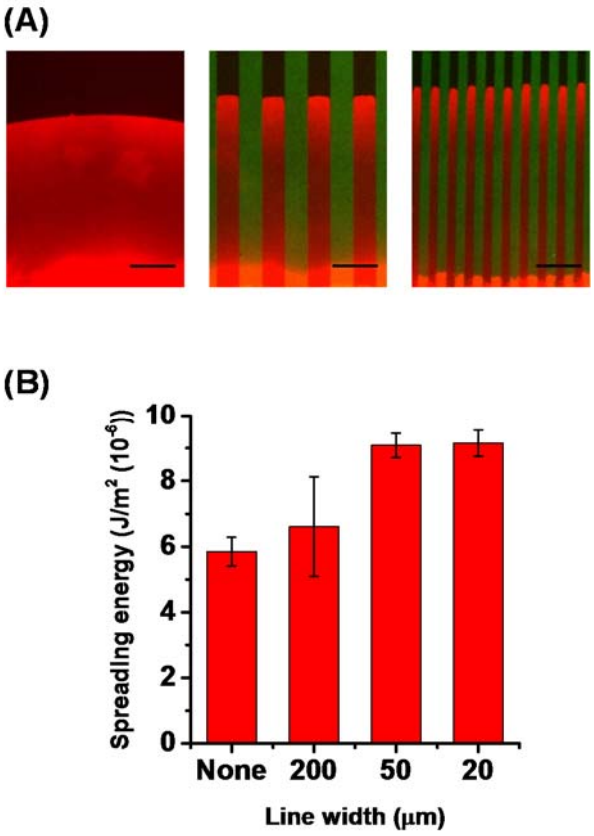

Figure 2: The effect of polymeric bilayer on the spreading velocity. (A) Fluorescence micrographs of self-spreading bilayers (DOPC/ TR-PE) on bare glass (left), line-patterned polymeric bilayers with the channel width of 50 μm (middle) and 20 μm (right). The red and green fluorescence were from DOPC/TR-PE and polymeric bilayers, respectively. (B) The spreading energy, W_A (Jm^{-2}), was compared for non-patterned cover glass and patterned polymeric bilayers with varied channel width.

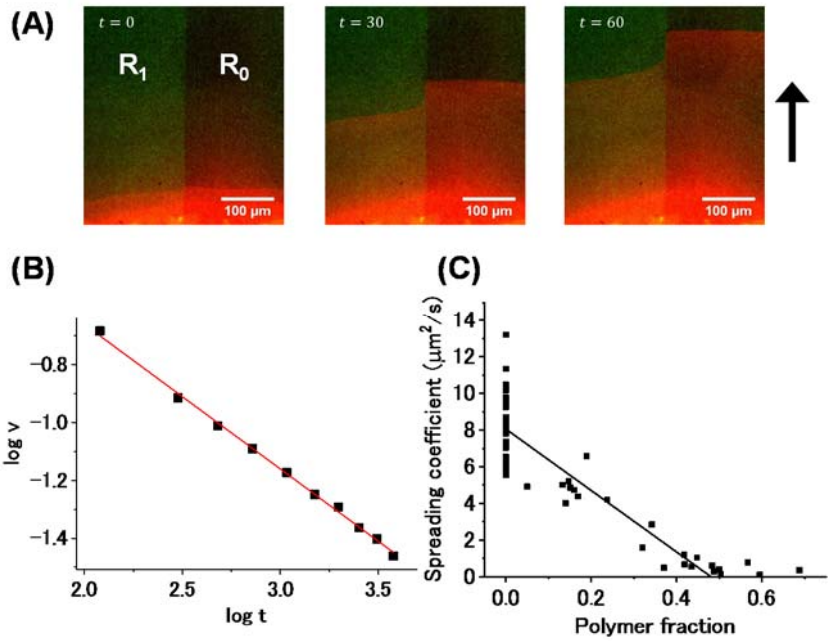

Figure 3: Self-spreading in the presence of polymerized bilayer domains. (A) Fluorescence micrographs of DOPC/TR-PE bilayer on a glass substrate having partially-polymerized-bilayer (R_1) and bilayer-free (R_0) regions. The red and green fluorescence are from DOPC/TR-PE and polymeric bilayer, respectively. The direction of spreading is indicated with an arrow. (B) A double logarithmic plot of the spreading velocity (μm/sec) versus time (sec) in R_1. The data points were fitted with the slope of -0.5 (red line). (C) The spreading coefficients were plotted versus the polymer fraction in R_1. Each dot represents the result of an independent sample having varied polymer fraction. A linear fitting line (black) shows the percolation behavior.

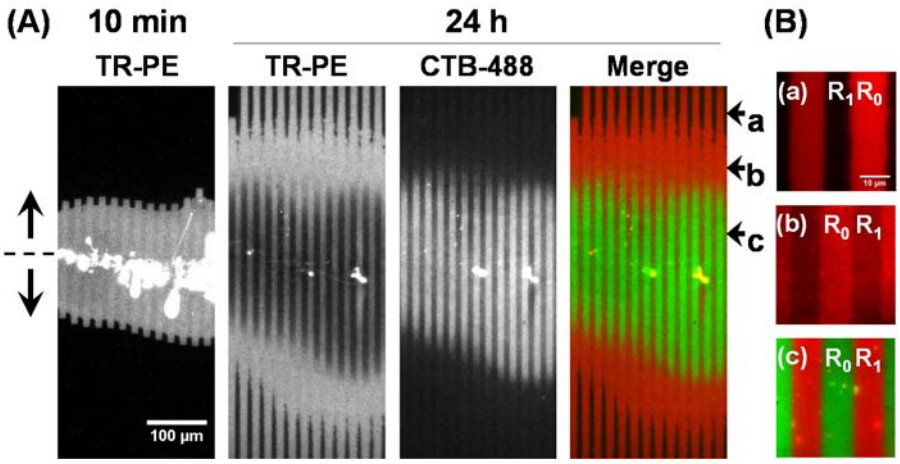

Figure 4: Phase separation in self-spreading bilayers. (A) Fluorescence micrographs of self-spreading bilayers on a glass substrate with partially-polymerized-bilayer (R_1) and bilayer-free (R_0) regions. Bilayers were composed of DOPC/ DPPC/ cholesterol (1:1:1) supplemented with 1mol% G_{M1} and 1mol% TR-PE. The lipid bilayers spread in two directions (upwards and downwards) from the lipid reservoir (indicated with a dashed line and arrows in the left side). The fluorescence micrographs of TR-PE were obtained at 10 min and 24 h after hydration. TR-PE primarily partitioned in L_d domains. The lipid reservoir had mostly disappeared after 24 h. CTB-488 was added afterwards to detect L_o domains. The fluorescence of TR-PE (left) and CTB-488 (center) were clearly separated (the merged image in the right shows TR-PE (red) and CTB-488 (green)). (B) Magnified images at three locations (indicated with arrows in (A) (a-c)).

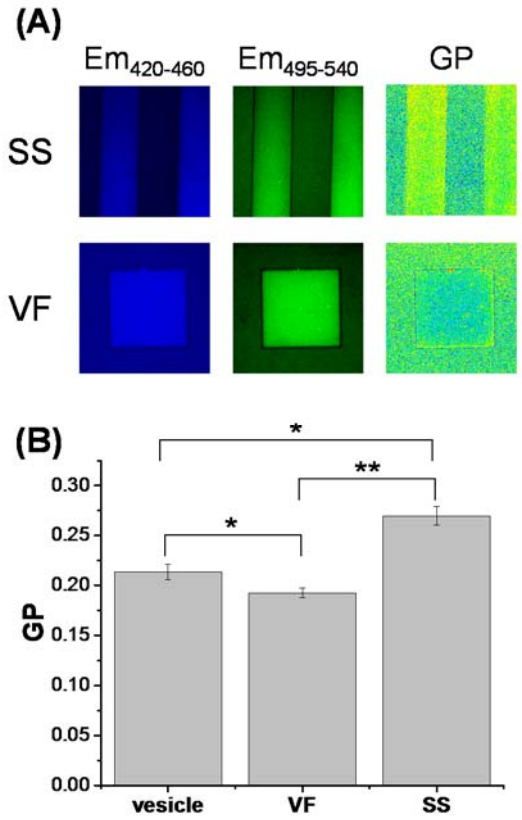

Figure 5: Lipid packing was evaluated with Laurdan for vesicles and supported membranes formed by self-spreading (SS) and vesicle fusion (VF). (A) Fluorescence of Laurdan in DOPC bilayers was observed in two spectral regions, *i.e.* 420–460 nm ($Em_{420-460}$) and 495–540 nm ($Em_{495-540}$), and the GP values were evaluated for each pixel. A brighter yellow color represents a higher GP value. A line pattern and a grid-shaped pattern (pattern size: 20 μm) were used for the supported membranes prepared by the self-spreading and vesicle fusion, respectively. (B) Average and standard error of GP were compared for bilayers in vesicles and supported membranes formed via vesicle fusion (VF) and self-spreading (SS). * $P<0.05$, ** $P<0.01$.

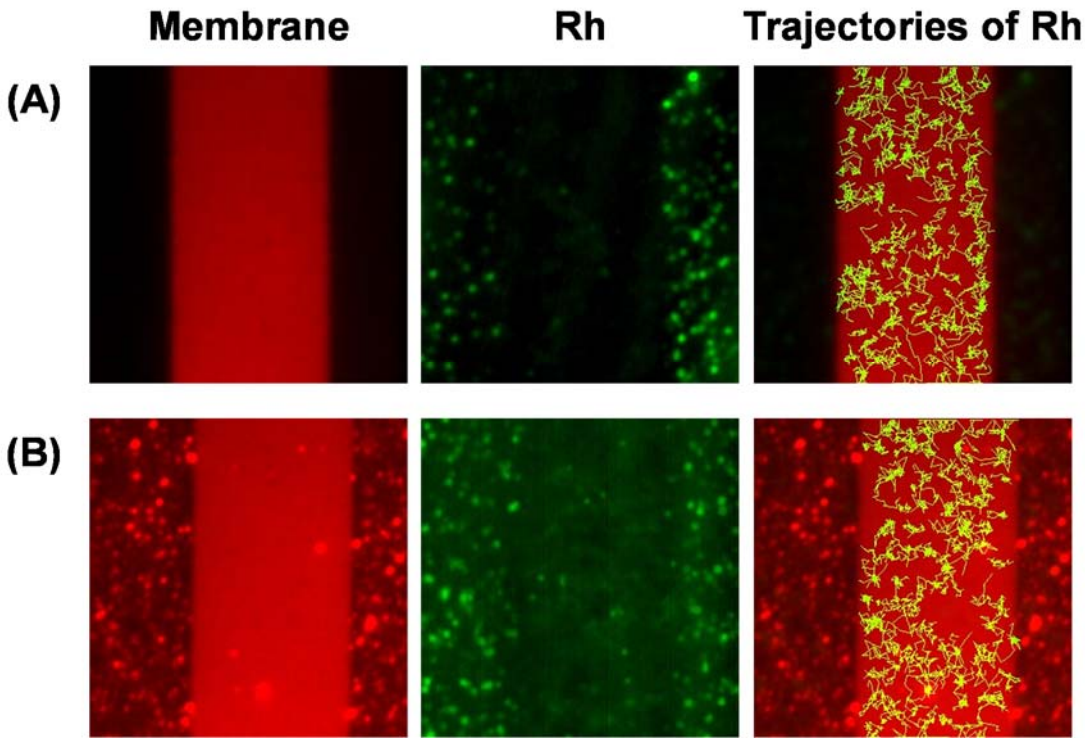

Figure 6: Reconstitution of Cy7-Rh in supported bilayers formed by self-spreading (A) and vesicle fusion (B). Left and center images are fluorescence from the lipid membrane (DOPC/ TR-PE) and Cy7-Rh, respectively. The right images are the overlay of fluorescence from DOPC/ TR-PE and trajectories of Cy7-Rh in the fluid bilayer. Laterally mobile Cy7-Rh molecules were observed in the fluid bilayer regions, whereas Cy7-Rh molecules in the polymeric bilayer region were mostly immobile (see Supporting Movies).

References:

(1) Sackmann, E. Supported membranes: scientific and practical applications. *Science (Washington)* **1996**, *271*, 43-48.

(2) Tanaka, M.; Sackmann, E. Polymer-supported membranes as models of the cell surface. *Nature* **2005**, *437*, 656-663.

(3) Castellana, E. T.; Cremer, P. S. Solid supported lipid bilayers: From biophysical studies to sensor design. *Surf. Sci. Rep.* **2006**, *61*, 429-444.

(4) Brian, A. A.; McConnell, H. M. Allogeneic stimulation of cytotoxic T cells by supported planar membranes. *Proc. Natl. Acad. Sci. USA* **1984**, *81*, 6159-6163.

(5) Reimhult, E.; Höök, F.; Kasemo, B. Intact vesicle adsorption and supported biomembrane formation from vesicles in solution: influence of surface chemistry, vesicle size, temperature, and osmotic pressure. *Langmuir* **2003**, *19*, 1681-1691.

(6) Richter, R. P.; Berat, R.; Brisson, A. R. Formation of solid-supported lipid bilayers: An integrated view. *Langmuir* **2006**, *22*, 3497-3505.

(7) Rädler, J.; Strey, H.; Sackmann, E. Phenomenology and kinetics of lipid bilayer spreading on hydrophilic surfaces. *Langmuir* **1995**, *11*, 4539-4548.

(8) Nissen, J.; Gritsch, S.; Wiegand, G.; Rädler, J. O. Wetting of phospholipid membranes on hydrophilic surfaces - Concepts towards self-healing membranes. *Euro. Phys. J. B* **1999**, *10*, 335-344.

(9) Nissen, J.; Jacobs, K.; Rädler, J. O. Interface dynamics of lipid membrane spreading on solid surfaces. *Phys. Rev. Lett.* **2001**, *86*, 1904-1907.

(10) Morigaki, K.; Baumgart, T.; Offenhäusser, A.; Knoll, W. Patterning solid-supported lipid bilayer membranes by lithographic polymerization of a diacetylene lipid. *Angew. Chem., Int. Ed.* **2001**, *40*, 172-174.

(11) Okazaki, T.; Inaba, T.; Tatsu, Y.; Tero, R.; Urisu, T.; Morigaki, K. Polymerized lipid bilayers on solid substrate: Morphologies and obstruction of lateral diffusion. *Langmuir* **2009**, *25*, 345-351.

(12) Okazaki, T.; Morigaki, K.; Taguchi, T. Phospholipid vesicle fusion on micropatterned polymeric bilayer substrates. *Biophys. J.* **2006**, *91*, 1757-1766.

(13) Suzuki, K.; Masuhara, H. Groove-spanning behavior of lipid membranes on microfabricated silicon substrates. *Langmuir* **2005**, *21*, 6487-6494.

(14) Furukawa, K.; Nakashima, H.; Kashimura, Y.; Torimitsu, K. Microchannel device using self-spreading lipid bilayer as molecule carrier. *Lab Chip* **2006**, *6*, 1001-1006.

(15) Furukawa, K.; Aiba, T. Supported lipid bilayer composition microarray fabricated by pattern-guided self-spreading. *Langmuir* **2011**, *27*, 7341-7344.

(16) Nabika, H.; Sasaki, A.; Takimoto, B.; Sawai, Y.; He, S.; Murakoshi, K. Controlling molecular diffusion in self-spreading lipid bilayer using periodic array of ultra-small metallic architecture on solid surface. *J. Am. Chem. Soc.* **2005**, *127*, 16786-16787.

(17) Morigaki, K.; Schönherr, H.; Okazaki, T. Polymerization of diacetylene phospholipid bilayers on solid substrate: Influence of the film deposition temperature *Langmuir* **2007**, *23*, 12254-12260.

(18) Parasassi, T.; Krasnowska, E. K.; Bagatolli, L.; Gratton, E. LAURDAN and PRODAN as polarity-sensitive fluorescent membrane probes. *J. Fluoresc.* **1998**, *8*, 365-373.

(19) Parasassi, T.; Stasio, G. D.; d'Ubaldo, A.; Gratton, E. Phase fluctuation in phospholipid membranes revealed by Laurdan fluorescence. *Biophys. J.* **1990**, *57*, 1179-1186.

(20) Ma, Y.; Benda, A.; Kwiatek, J.; Owen, D. M.; Gaus, K. Time-resolved Laurdan fluorescence reveals insights into membrane viscosity and hydration levels.

Biophys. J. **2018**, *115*, 1498-1508.

(21) Dodes Traian, M. M.; Gonzalez Flecha, F. L.; Levi, V. Imaging lipid lateral organization in membranes with C-laurdan in a confocal microscope. *J. Lipid Res.* **2012**, *53*, 609-616.

(22) Hayashi, F.; Yamazaki, A. Polymorphism in purified guanylate cyclase from vertebrate rod photoreceptors. *Proc. Natl. Acad. Sci. U. S. A.* **1991**, *88*, 4746-4750.

(23) Litman, B. J. Purification of rhodopsin by concanavalin A affinity chromatography. *Meth. Enzymol.* **1982**, *81*, 150-153.

(24) Tanimoto, Y.; Okada, K.; Hayashi, F.; Morigaki, K. Evaluating the raftophilicity of rhodopsin photoreceptor in a patterned model membrane. *Biophys. J.* **2015**, *109*, 2307-2316.

(25) Sanii, B.; Parikh, A. N. Surface-energy dependent spreading of lipid monolayers and bilayers. *Soft Matter* **2007**, *3*, 974-977.

(26) Israelachvili, J. *Intermolecular & Surface Forces*; 3rd. Ed. ed.; Academic Press: London, 2011.

(27) Rehfeld, S. J. Adsorption of sodium dodecyl sulfate at various hydrocarbon-water interfaces. *J. Phys. Chem.* **1967**, *71*, 738-745.

(28) Saxton, M. J. Lateral diffusion in an archipelago: effects of impermeable patches on diffusion in a cell membrane. *Biophys. J.* **1982**, *39*, 165-173.

(29) Saxton, M. J. Two-dimensional continuum percolation threshold for diffusing particles of nonzero radius. *Biophys. J.* **2010**, *99*, 1490-1499.

(30) Lingwood, D.; Simons, K. Lipid rafts as a membrane-organizing principle. *Science* **2010**, *327*, 46-50.

(31) Kusumi, A.; Fujiwara, T. K.; Chadda, R.; Xie, M.; Tsunoyama, T. A.; Kalay, Z.; Kasai, R. S.; Suzuki, K. G. N. Dynamic organizing principles of the plasma

membrane that regulate signal transduction: Commemorating the fortieth anniversary of Singer and Nicolson's fluid-mosaic model. *Annu. Rev. Cell Dev. Biol.* **2012**, *28*, 215-250.

(32) Veatch, S. L.; Keller, S. L. Separation of liquid phases in giant vesicles of ternary mixtures of phospholipids and cholesterol. *Biophys. J.* **2003**, *85*, 3074-3083.

(33) Baumgart, T.; Hess, S. T.; Webb, W. W. Imaging coexisting fluid domains in biomembrane models coupling curvature and line tension. *Nature* **2003**, *425*, 821-824.

(34) Dietrich, C.; Bagatolli, L. A.; Volovyk, Z. N.; Thompson, N. L.; Levi, M.; Jacobson, K.; Gratton, E. Lipid rafts reconstituted in model membranes. *Biophys. J.* **2001**, *80*, 1417-1428. .

(35) Yoon, T.-Y.; Jeong, C.; Lee, S.-W.; Kim, J. H.; Choi, M. C.; Kim, S.-J.; Kim, M. W.; Lee, S.-D. Topographic control of lipid-raft reconstitution in model membranes. *Nat. Mat.* **2006**, *5*, 281-285.

(36) Roder, F.; Birkholz, O.; Beutel, O.; Paterok, D.; Piehler, J. Spatial organization of lipid phases in micropatterned polymer-supported membranes. *J. Am. Chem. Soc.* **2013**, *135*, 1189-1192.

(37) Okazaki, T.; Tatsu, Y.; Morigaki, K. Phase separation of lipid microdomains controlled by polymerized lipid bilayer matrices. *Langmuir* **2010**, *26*, 4126-4129.

(38) Yokota, K.; Toyoki, A.; Yamazaki, K.; Ogino, T. Behavior of raft-like domain in stacked structures of ternary lipid bilayers prepared by self-spreading method. *Jpn. J. Appl. Phys.* **2014**, *53*, 05FA11.

(39) Morigaki, K.; Tawa, K. Vesicle fusion studied by surface plasmon resonance and surface plasmon fluorescence spectroscopy. *Biophys. J.* **2006**, *91*, 1380-1387.

TOC:

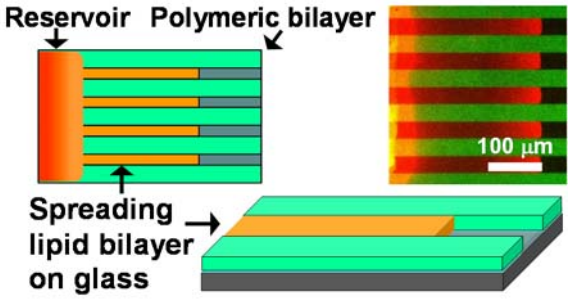
Reservoir
Polymeric bilayer
100 μm
Spreading
lipid bilayer
on glass